PHYSICAL ASPECTS OF ELECTRO-OPTIC PROPERTIES OF SMECTIC LIQUID CRYSTALS

P. E. CLADIS[1,2] and H. R. BRAND[2,1]

1. Bell Laboratories, Lucent Technologies, Murray Hill, NJ 07974, USA

2. Theoretische Physik III, Universität Bayreuth, D-95440 Bayreuth, Germany

Abstract

We present an *Effective Internal Field Model* for the antiferroelectric (AF) to field induced ferroelectric (FF) transition of smectic C_A. This model attributes the fast dynamics and high threshold fields of this transition to the large magnitudes of its in-plane polarization. We conclude that propagating fingers observed in the vicinity of the $AF \leftrightarrow FF$ threshold field can only be observed in holding fields where there are metastable states. We argue that this is because relaxation times for antiferroelectric liquid crystals (AFLCs) are too fast ($\sim \mu s$) for front propagation of stable states into unstable ones. The model is also used to interpret the decrease in threshold field when smectic C* is added to C_A.

Keywords: Chiral Smectics: helielectric, antiferroelectric, ferroelectric liquid crystals; electro-optic properties, passive liquid crystal displays

Introduction

Since the discovery of the transistor, one of the most impressive technical triumphs has been the development by colleagues in Japan of active matrix liquid crystal displays. Because of the cooperative physical properties of nematic liquid crystals, AMLCDs are light-weight, low power consuming and fast. Most importantly, their visual impact is stunning. Indeed, AMLCDs are now the display technology to beat.

Manufacturing AMLCDs is expensive. It also requires a critical workforce skilled in mass production of semiconductor devices. While the liquid crystal display market is large (over $8 billion annually), its profit margin

is slim. As a result, Japan is still the country that over-whelmingly dominates AMLCD mass production and development. However, as displays are a strategic component in advanced electronic products, there are considerable business pressures to find new display technologies that, while less costly to produce, have display characteristics comparable to (or better than) the state of the art AMLCDs.

One strategy to address these interests has been to explore passive liquid crystal display technologies. Particularly successful passive technologies have resulted using chiral smectic liquid crystals; first smectic C*, known as ferroelectric liquid crystals (FLCs) [1] and, most recently, smectic C_A, known as antiferroelectric liquid crystals (AFLCs) [2].

Display interest in smectics was first triggered by a classical symmetry argument predicting the possibility of a spontaneous polarization, $\mathbf{P}_o$, perpendicular to the tilt plane in a single layer of chiral smectic C (smectic C*) [3]. However, the observation is that while one layer is ferroelectric, in the case of many layers, $\mathbf{P}_o$ rotates uniformly about the layer normal. As a result, bulk properties of smectic C* (and chiral smectics that are fluid in the plane of the layers) are helielectric [4] rather than ferroelectric. A consequence of the 2π degeneracy of $\mathbf{P}_o$ in helielectrics - i.e. smectic C*, in particular - is that there is no threshold for reversal of $\mathbf{P}_o$ when an external DC electric field changes sign [5].

By preparing very thin samples to suppress the smectic C* helix structure with surface forces, a viable "flicker free" passive display technology was invented [1, 6]. This technology is called *Surface Stabilized Ferroelectric Liquid Crystals* (SSFLC) [6]. Today SSFLC's are well-positioned to replace bulky power-hungry cathode ray tubes now used in work-stations for e.g. desk-top publishing.

FLCDs/SSFLCs rely on the fact that when $\mathbf{P}_o$ is reversed by changing the sign of a DC applied electric field, the liquid crystal director (optic axis) rotates through $2\theta \sim 45°$, where θ is the molecular tilt in the layers. As viewed between crossed polarizers, a dark state can be observed by setting the extinction direction for one sign of the field resulting in a maximally bright state for the other. Because liquid crystal elastic torques are tiny in comparison to torques from electric fields, an FLCD pixel can be either "off" or "on". However, while FLCDs have no gray scale, multi-color FLCDs have been achieved using 5 color sub-pixels, rather than the usual 3 (RGB) of AMLCDs. As there is no threshold associated with the smectic C* electro-optic effect, novel ways to drive SSFLC's had to be invented. In addition, fighting "sticky" surface forces tends to make FLCDs slow - today, still only "nearly video-rate" with a relatively large power consumption (about 50W) compared to AMLCDs (less than 1W). Lastly, because of their sensitivity to surface conditions, FLCDs require a shock-proof environment to operate. All these features of FLCDs are predictable from the physical properties of

smectic C* and solvable by clever engineering.

The recent discovery of antiferroelectric liquid crystals (smectic C_A) [7] led quickly to the realization of a full-color, video-rate passive display technology (AFLCDs) with a uniformly large viewing angle [8]. In AFLCs, the molecular tilt in one layer is equal and opposite to that of adjacent layers ($\pm\theta$). In bulk C_A there is also a macroscopic helix structure involving two helices out of phase by π [9]. In both cases, the optic axis coincides with the layer normal. Above a relatively large threshold field, E_{thr}, there is a transition from the antiferroelectric state (AF) to a field induced ferroelectric one (FF) where the molecular tilt is the same in all layers [9]. This implies a rotation in the optic axis by θ relative to the AF state.

Figure 1: FF fingers (bright) propagating into the AF state (dark) observed between polarizer (P) and analyzer (A) by JianFeng Li [12]. The material is TFMHOBC with rubbed polyimide (DuPont PI2550) surface treatment. The fingers propagate parallel to the layers i.e. parallel to the top and bottom edges of the snapshot. The temperature is $110°C$, sample thickness $\sim 8\mu m$. 200X magnification.

Since the $AF \leftrightarrow FF$ transition is hysteretic, multiplexing schemes can be used to drive AFLCDs [10]. Because the transition does not take place uniformly but rather as micron width fingers of one state rapidly propagating parallel to the layer into the other state, AFLCDs have a gray scale [11]. Fig. 1 is a snapshot of the propagating fingers [12]. The dynamics of the $AF \leftrightarrow FF$ propagating fingers was studied in the vicinity of E_{thr} by Li et al. [13]. In contrast to the liquid crystal state used in AMLCDs (nematic liquid crystals), E_{thr}, is rather large in AFLCs. To understand if this is an intrinsic property of AFLCs or a feature that can be controlled to optimize display performance, we need to develop a more physical picture of the

$AF \leftrightarrow FF$ transition.

Recently, Inui et al. [14] showed that E_{thr} could be reduced by adding increasing concentrations of a material with a C* phase (which has no threshold) to one with a C_A phase. At sufficiently large doses of C*, the idea was that a *thresholdless antiferroelectric* transition (TLAF) could eventually take place. Their hypothesis is that TLAF occurs when the direction of $\mathbf{P}_o$ is uncorrelated from layer to layer so that the $AF \leftrightarrow FF$ transition occurs continuously without propagating fingers and there is no helix structure. Here, we discuss an *Effective Internal Field Model* to improve our understanding of TLAF, in particular, and AFLCs in general.

While the picture that emerges may help engineer better AFLCDs, we consider it only one of the many fascinating aspects of AFLCs that need to be addressed to develop better physical insight into this novel state of nature. For example, we would like to know what are important parameters setting the finger widths and how these are related to the uniformity of the AFLCD viewing angle. Are finger widths determined by the surface treatment? The helix structure? Another important but still unclear aspect is the origin of the high speeds involved at the $AF \leftrightarrow FF$ transition and the nature of its dynamics (propagative or diffusive) far from E_{thr}.

An Effective Internal Field Model

To simplify the discussion, we ignore the macroscopic helix structure of AFLCs. The assumption is that this does not affect conclusions drawn concerning the magnitude for E_{thr} nor the dynamics of the field induced $AF \leftrightarrow FF$ transition. Values for the material constants used here are those taken from Li et al. [13].

In the model (Fig. 2) we consider one smectic layer (designated layer 1) with an in-plane polarization, $\mathbf{P}_1$. The layer normal is taken to be along $\hat{z}$. Angles in the plane perpendicular to $\hat{z}$ are denoted by ϕ and those on a cone around $\hat{z}$ by θ (Fig. 2). In the (ϕ, θ) reference frame, the antiferroelectric orientation of $\mathbf{P}_1$ is $(0,\ \pi/2)$. When $E > E_{thr}$, $\mathbf{P}_1$ rotates in the plane perpendicular to $\hat{z}$ so that $\mathbf{P}_1 \parallel \mathbf{E}$: i.e. at the $AF \rightarrow FF$ transition, $(0,\ \pi/2) \rightarrow (\pi,\ \pi/2)$.

We model the internal fields from all the other layers "seen" by layer 1 with an effective internal field, $\mathbf{E}_{int}^{eff} = \beta \mathbf{P}_2$. That is, we think of a two layer model with the second layer taking the place of all the other layers with its polarization vector, $\mathbf{P}_2 = -\mathbf{P}_1$, in the AF state. Call the coupling constant controling the interaction between the two layers β. When $\beta > 0$, the energy density from this coupling is $\beta \mathbf{P}_1 \cdot \mathbf{P}_2 = \beta P_o^2 \cos\phi$, where ϕ is the angle between $\mathbf{P}_1$ and $\mathbf{P}_2$. This energy density is minimum when $\phi = \pi$ [15]. In the AF state, we put P_2 parallel to an applied electric field, E: $\mathbf{P_2} \parallel \mathbf{E}$ and $\mathbf{P}_1$ antiparallel to $\mathbf{E}$. The director (optic axis) orientation in both layers is

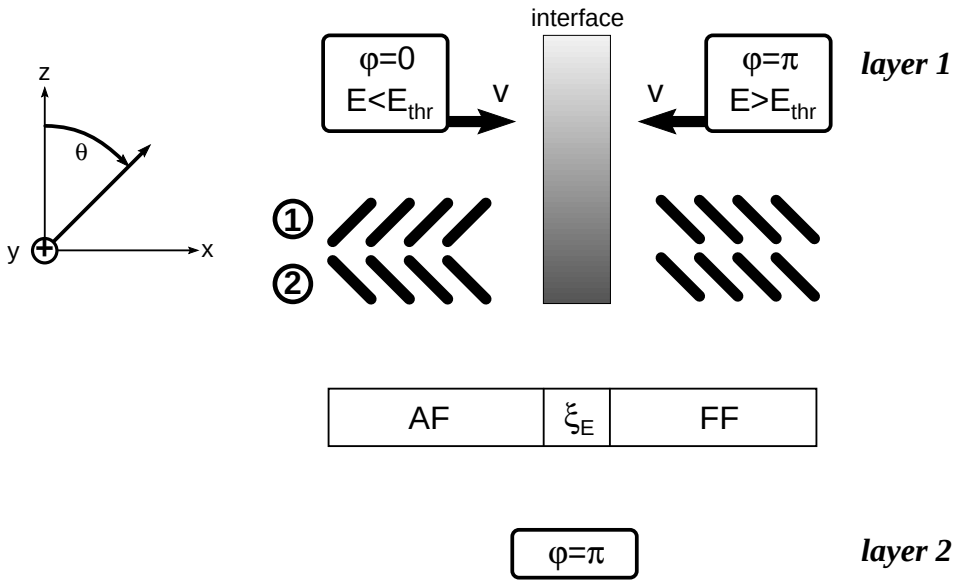

Figure 2: Reference frame for the *Effective Internal Field Model*. ξ_E is a measure of the AF-FF interface width. The interface travels with velocity v in the direction shown by the appropriate arrows depending on whether E is above or below E_{thr}.

at a constant θ assumed independent of E. In the AF state, $\phi_1 = 0$ in layer 1 and $\phi_2 = \pi$ in layer 2. In the FF state, $\phi_1 = \phi_2 = \pi$ (Fig. 2).

The picture is that in the AF state, an internal effective field forces $\mathbf{P}_1$ to be antiparallel to $\mathbf{P}_2$. The electro-optic effect involved in the $AF \rightarrow FF$ transition results when the applied field overcomes the internal field thus allowing $\phi_1 \rightarrow \pi = \phi_2$.

The free energy density, f_1, for layer 1 is modeled with the following terms:

$$f_1 = \begin{cases} \frac{1}{2}K \sin^2\theta \left(\frac{\partial\phi}{\partial x}\right)^2 & \text{elasticity} \\ -\frac{\varepsilon_c \sin^2\theta}{8\pi} E^2 \sin^2\phi & \text{dielectric coupling} \\ -\mathbf{P_1}\cdot\mathbf{E} & \text{ferroelectric coupling} \\ +\beta\mathbf{P_1}\cdot\mathbf{P_2} & \text{coupling to layer 2} \end{cases} \quad (1)$$

where elasticity refers to the energy required to create spatial variations in ϕ in layer 1. This is determined by the magnitude of the effective elastic constant in a layer, $K \sim 10^{-6} dyn$, and the molecular tilt in a layer, $\theta \sim 20°$. The dielectric coupling to the applied field, E, depends on the sign of the dielectric anisotropy, ε_c, within a layer. When $\varepsilon_c < 0$, both $\phi = 0$ and $\phi = \pi$ are stable - the director is oriented perpendicular to $\mathbf{E}$. The situation is

more complex when $\varepsilon_c > 0$ and may even involve distortions in the layer configuration.

The ferroelectric coupling is minimal when $\mathbf{P_1} \parallel \mathbf{E}$. When $\beta > 0$, the coupling term between $\mathbf{P_1}$ and $\mathbf{P_2}$ decreases f_1 most when $\phi = \pi$. The situation where $\mathbf{P_1}$ is independent of $\mathbf{P_2}$ is described by $\beta = 0$. We identify this case with TLAF [14] for which there is no correlation between the polarization vectors in neighboring layers. A ferroelectric coupling between P_1 and P_2 implies $\beta < 0$, *i.e.* $\mathbf{P_1} \parallel \mathbf{P_2}$ in the absence of E. But as our ansatz is that $\mathbf{P_1}$ is initially antiparallel to $\mathbf{E}$, the ferroelectric case ($\beta < 0$) is not included in this model.

To reveal the dynamics, the minimizer of the free energy is equated to the time dependence of ϕ, *i.e.* $\delta f_1 = \gamma_c \dfrac{\partial \phi}{\partial t}$ where $\gamma_c \sim 0.25 poise$ [13] is the viscosity for the director rotation in layer 1.

$$\gamma_c \frac{\partial \phi}{\partial t} = K \sin^2\theta \frac{\partial^2 \phi}{\partial x^2} + \frac{\varepsilon_c \sin^2\theta}{4\pi} E^2 \sin\phi\cos\phi - P_o E \sin\phi + \beta P_o^2 \sin\phi \quad . \quad (2)$$

Next we transform to traveling coordinates: $u = x - vt$, and define the usual electric coherence length (the characteristic length for ϕ to change from 0 to π (Fig. 2)):

$$\xi_E = \left(-\frac{4\pi K}{\varepsilon_c E^2}\right)^{1/2} \sim 600 \text{ Å} \qquad \rightarrow \varepsilon_c < 0$$

to get

$$\frac{d^2\phi}{du^2} - \frac{1}{\xi_E^2}\sin\phi\cos\phi = \frac{-v\gamma_c}{K\sin^2\theta}\left(\frac{d\phi}{du}\right) + \frac{P_o(E - \beta P_o)}{K\sin^2\theta}\sin\phi \quad . \quad (3)$$

The terms in Eq. 3 are grouped to show that the right hand side is the first integral of the left hand side when the constant of integration is zero. The physical interpretation of this choice of integration constant is that the driving force,

$$\frac{P_o(E - \beta P_o)}{K\sin^2\theta}\sin\phi \quad ,$$

goes only into dissipation at the traveling interface:

$$\frac{-v\gamma_c}{K\sin^2\theta}\left(\frac{d\phi}{du}\right) \quad .$$

When the layer dielectric anisotropy $\varepsilon_c < 0$, the dielectric energy compensates for the increase in elastic energy created at the AF-FF traveling interface.

A solitary wave solution [16] is:

$$\phi = 2\arctan(\exp(x - vt)/\xi_E) \quad ,$$

if, and only if, $\varepsilon_c < 0$. Equating coefficients we obtain, the speed of the propagating finger, v, as

$$v = \xi_E(E - \beta P_o)\frac{P_o}{\gamma_c} = v_o\frac{E - E_{thr}}{E}$$

showing the observed [13] linear dependence on E when $E \sim E_{thr} = \beta P_o$, the effective field from layer 2. When $\beta \leq 0$, a threshold field cannot be defined. As $E \to \infty$, then $v \to v_o \sim 3cm/s$ which agrees with observations for a compound where $\beta \sim 1$ [13].

An interesting limit of this model is where $\varepsilon_c \to 0^-$. In this case, layer 1 does not have to fight so hard against the stabilizing dielectric torques (Eq. 2). Thus, while the interface between the AF and FF regions expands, it also travels faster. This suggests that even faster antiferroelectric devices may be obtained by choosing materials with $\varepsilon_c \lesssim 0$.

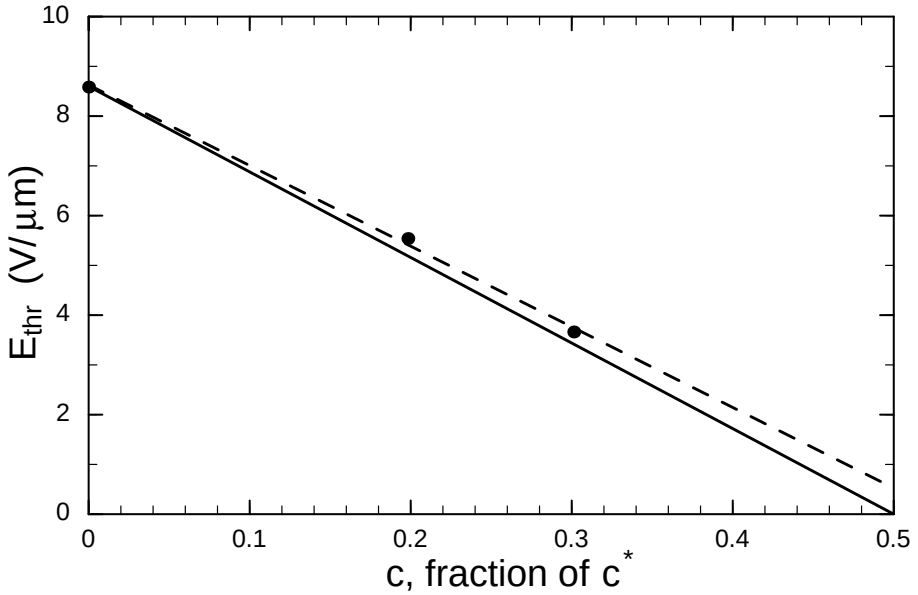

Figure 3: E_{thr} vs. concentration of C* in C_A. The solid line is the prediction of the model discussed here assuming $\beta = 1$ for C_A and $\beta = -1$ for C*. The dashed line is the best fit through the observed points [14].

Another interesting limit addresses the results of TLAF [14]. In this paper, the authors show that mixing a compound with a smectic C* phase with one having a C_A phase results in a mixture with a reduced threshold field (Fig. 3). Furthermore, the reduction in E_{thr} appears to a good approximation to be linear in concentration, c, up to $c \sim 30\%$ of the C* material. Assuming that the interactions between the two compounds are "short range" over the observed concentration range, a lowest order estimate of the effective threshold field suggests that, certainly at small concentrations, adding *e.g.* $c = 30\%$ of a smectic C* compound with $E_{thr} = 0$ to

an antiferroelectric one with $E_{thr}(c=0) = E^o_{thr} = 8.6V/\mu m$, should result in a mixture with an effective threshold field that is given by a weighted average of the two threshold fields: $E^{eff}_{thr} = 0.7 \times E^o_{thr} = 6.0V/\mu m$. Instead, for this mixture, the observed threshold field is smaller by nearly a factor of 2: $E^{obs}_{thr} = 3.7V/\mu m$ (Fig. 3). Can we understand this discrepancy?

Going back to Eq. 1, we note that the effective internal field model stresses macroscopic features of the $AF \leftrightarrow FF$ transition, i.e. involves long range cooperative interactions between layer 1 and all the other layers. In this context, the argument we propose is that adding $c = 30\%$ of a material with a $\beta = -1$ (smectic C*) to one with $\beta = +1$ (smectic C_A), results in an effective β, $\beta_{eff} = 0.7 \times 1 + 0.3 \times (-1) = (1 - 2c) = 0.4$. In which case, the prediction would be $E^{eff}_{thr} = \beta_{eff} \times E^o_{thr} = 3.6V/\mu m$ which is much closer (Fig. 3) to the observed results [14]. The conclusion is that interactions involved in C*/C_A mixtures have significant medium to long range features.

Stability

The fact that the finger speed is observed to be linear in E going through zero when $E = E_{thr}$, implies that the $AF \leftrightarrow FF$ transition is first order [17]. In the case of a first order transition, the speed of a front propagating from a metastable state into a stable state is unique. In Eq. 2, the interface is traveling in a potential, V_o, given by:

$$V_o = P_o^2 \left((1 - e) \cos\phi - \delta e^2 \cos 2\phi \right)$$

where $e = \dfrac{E}{\beta P_o}$ and $\delta = \dfrac{|\epsilon_c| \sin^2\theta}{16\pi}$. V_o has extrema for $\phi = 0$ and $\phi = \pi$. The windows where there are stable and metastable states are $1 - 4\delta < e < 1 + 4\delta$ and $1/4\delta < e < \infty$ as $\delta \sim 2.3 \times 10^{-3}$ or with the values of Li et al. [13]: $0.9 < e < 1.01$ and $400 < e < \infty$, respectively. Assuming the material shows no dielectric breakdown in a field $\sim 4kV/\mu m$, the high field metastable region raises the possibility of directly observing $v_o \sim 3cm/s$ [13].

What happens when the field is turned off in the FF state? Does layer 1 relax from $\phi = \pi$ to $\phi = 0$ faster than the AF state can propagate into an unstable FF state at the marginally stable [18, 19] expected rate [13]?

Here we argue that, given the fast characteristic times of AFLCs, the FF state can relax to the AF state before a front has a chance to propagate from an unstable FF state into the stable AF state. To see this, we put $E \to 0$ in Eq. 2 and transform to dimensionless units. A characteristic time, $\tau = \gamma_c/\beta P_o^2 = 5\mu s$ and a characteristic length, $x_o = \sqrt{K} \sin\theta/\sqrt{\beta} P_o \sim 152$ Å can be defined. The marginally stable speed [18, 19, 20] for front propagation is then $2x_o/\tau = 0.6cm/s < v_o$.

Suppose when $E \to 0$, $\phi = \pi$ everywhere and the system is unstable. A

small fluctuation in ϕ, $\pm\delta\phi_o$, then grows as

$$tan\left(\frac{\phi-\pi}{2}\right) = \pm tan\left(\frac{\delta\phi_o}{2}\right)\exp(\frac{t}{\tau}) \quad . \tag{4}$$

A tiny $\delta\phi_o \sim 0.1^\circ$ relaxes $\phi \rightarrow 0$ in about $10\tau \sim 50\mu s$ and a $\delta\phi_o \sim 10^\circ$ in $\sim 4\tau \sim 20\mu s$, i.e. much faster than can be captured by a video-camera operating at $\sim 0.1s/frame$ [11]. In contrast, a marginally stable front travels $0.6mm$ in $0.1s$. As a result, for a field of view $\sim 1.5mm$, one can capture at least three video-frames showing the propagating $AF \rightarrow FF$ front. The observation is that the zero field $FF \rightarrow AF$ transition occurs faster than one video-frame [11]. Thus, we conclude that AFLCs with their large βP_o^2's enable the FF state to relax in zero field before an $FF \rightarrow AF$ front can form and propagate.

Conclusions

In the Effective Internal Field Model, the fast dynamics and the large E_{thr} of AFLCs is directly related to its large value for P_o. Adding smectic C* materials to smectic C_A should have the effect of both reducing E_{thr} and slowing the C_A electrooptic effect. For fields outside the region where there are metastable states, we expect that $AF \leftrightarrow FF$ dynamics will be controlled by the relaxation mechanism described in Eq. 4 rather than finger propagation.

Acknowledgments

We thank F. Schmögner for help with the figures and J-F. Li for Fig. 1. P.E.C. thanks the Alexander von Humboldt Foundation for an AvH Research Award, Advanced Liquid Crystal Technologies, Inc. for partial support and the Universität Bayreuth for hospitality.

References

[1] N. A. Clark and S. T. Lagerwall, *Appl. Phys. Lett.* **36**, 899 (1980).

[2] Y. Yamada, N. Yamamoto, K. Mori, K. Nakamura, T. Hagiwara, Y. Suzuki, I. Kawamura, H. Orihara and Y. Ishibashi, *Jpn. J. Appl. Phys.*, **29** , 1757 (1990). The title of this paper is: *Ferroelectric Liquid Crystal Display Using Tristable Switching.* However, except for a succinct summary of technical problems associated with smectic C* display technology, it addresses the antiferroelectric liquid crystal display technology and includes a snapshot of (at that time) "The newest display in the world".

[3] R. B. Meyer, L. Liébert, L. Strzelecki and P. Keller, *J. Physique Lett.* **36** , L69 (1975).

[4] *See for example*: H. R. Brand and P. E. Cladis, *Mol. Cryst. Liq. Cryst.*, **114**, 207 (1984); H. R. Brand, P. E. Cladis and P. L. Finn, *Phys. Rev.* **A31** , 361 (1985).

[5] P. E. Cladis, H. R. Brand and P. L. Finn, *Phys. Rev.* **A28**, Rap. Comm. 512 (1983).

[6] S. T. Lagerwall and T. Dahl, *Mol. Cryst. Liq. Cryst.* **114**, 151 (1984).

[7] A. D. L. Chandani, T. Hagiwara, Y. Suzuki, Y. Ouchi, H. Takezoe and A. Fukuda, *Jpn. J. Appl. Phys.* **27**, L729 (1988)

[8] *See for example*: Y. Yamada, N. Yamamoto, K. Nakamura, N. Koshobu, S. Ohmi, R. Sato, K. Aoki and S. Imai, *SID 95 Digest*, p. 789 (1995); K. Nakamura, N. Koshoubu, N. Yamamoto, Y. Yamada, N. Okabe and Y. Suzuki, *Asia Display '95, Hammamatsu*, p. 69 (1995).

[9] *For a recent review*: A. Fukuda, Y. Takanishi, T. Isozaki, K. Ishikawa and H. Takezoe, *J. Mater. Chem.* **4**, 997 (1994).

[10] Y. Suzuki, T. Hagiwara, I. Kawamura, N. Okamura, T. Kitazume, M. Kakimoto, Y. Imai, Y. Ouchi, H. Takezoe and A. Fukuda, *Liq. Crystals,* **6**, 167 (1989).

[11] P. E. Cladis and H. R. Brand, *Liq. Cryst.* **14**, 1327 (1993).

[12] We thank Dr. JianFeng Li (Reveo, Inc.) for his dramatic snapshot of the propagating fingers (Fig. 1).

[13] J.F. Li, X.Y. Wang, E. Kangas, P. L. Taylor, C. Rosenblatt, Y. Suzuki and P. E. Cladis, *Phys. Rev.* **B52** *Rap. Comm.* R13075 (1995); *Mol. Cryst. Liq. Cryst.* **288**, 73 (1996).

[14] S. Inui, N. Iimura, T. Suzuki, H. Iwane, K. Miyachi, Y. Takanishi and A. Fukuda, *J. Mater. Chem.,* **6**, 671 (1996).

[15] Our model differs from previous ones (e.g. Ref. [13], M. Čepič and B. Žekš, *Mol. Cryst. Liq. Cryst.* **263**, 61 (1995)) only in that we identify the interlayer coupling called e.g. U/2 in Ref. [13] involving local dipole interactions and possible steric effects, as $\beta \mathbf{P_1} \cdot \mathbf{P_2}$, where $\mathbf{P_i}$ are the macroscopic polarizations associated with layer i.

[16] P. E. Cladis and W. van Saarloos in *Solitons in Liquid Crystals*, edited by L. Lam and J. Prost (Springer-Verlag, New York, 1992).

[17] P. E. Cladis, W. van Saarloos, D. A. Huse, J. S. Patel, J. W. Goodby and P. L. Finn, *Phy. Rev. Lett.,* **62**, 1764 (1989).

[18] G. Dee and J. S. Langer, *Phys. Rev. Lett.* **50**, 383 (1983).

[19] D.G. Aronson and H.F. Weinberger, *Adv.Math.* **30**, 33 (1978).

[20] E. Ben-Jacob, H.R. Brand, G. Dee, L. Kramer, and J.S.Langer, *Physica* **D14**, 348 (1985). These authors give the first discussion of Type II marginal stability used in Ref. [16] to discuss smectic C* when $E \neq 0$. The $E = 0$ case for C_A, is Type I marginal stability [18, 19].